

Analysis of final-state momentum distributions of ionization products in ion-atom collisions

Y. D. Wang,^{1,*} V. D. Rodríguez,^{2,†} C. D. Lin,^{3,‡} C. L. Cocke,¹ S. Kravis,¹ M. Abdallah,¹ and R. Dörner^{1,4}

¹*J. R. Macdonald Laboratory, Department of Physics, Kansas State University, Manhattan, Kansas 66506-2601*

²*Departamento de Física, Universidad de Buenos Aires, 1428 Buenos Aires, Argentina*

³*The Joint Institute for Laboratory Astrophysics, University of Colorado, Boulder, Colorado 80309-0440*

⁴*Institut für Kernphysik, Universität Frankfurt, D60486 Frankfurt, Germany*

(Received 2 November 1995)

A general formulation utilizing three-body kinematics was developed to analyze the final-state momentum distributions of the electron, the recoil, and the projectile ion, for the ionization process in ion-atom collisions. Information on ionization dynamics can be identified and analyzed from the perspective of momentum distributions. The mechanism of electron capture into the projectile continuum was found to contribute a finite value at the kinematical threshold in the longitudinal recoil-ion momentum distribution. Detailed calculations using the continuum distorted wave–eikonal initial state approximation are compared with two recent measurements on momentum distributions of the recoiling ion and the ionized electron in single ionization of He by protons and by highly charged projectiles.

PACS number(s): 34.10.+x, 34.50.Fa

I. INTRODUCTION

The ionization process in ion-atom collisions provides fertile ground to test our understanding and our ability to describe the breakup of basic Coulombic three-body systems. While much of our knowledge of ionization dynamics originates from the study of the ejected electron spectra and some from the projectile angular distributions, recent developments in recoil-ion momentum spectroscopy have added new dimensions for the detailed study of ion-atom collision dynamics. Momentum distributions of the recoiling ions and the electrons have been carried out in the last few years [1–7]. Together with the measurements of ejected electron spectra and the projectile angular distributions, these measurements offer a wealth of information on ionization dynamics and can serve as a stringent test for theory.

Most of the existing theoretical analysis on recoil-ion momentum distributions have been carried out using the n -body classical trajectory Monte Carlo method (n CTMC) [1,2,4–6]. The momentum distributions of the recoil ions, however, are not independent of the momentum distributions of the scattered projectiles and/or of the ejected electrons. In a recent paper, Rodríguez, Wang, and Lin [8] analyzed the longitudinal recoil-ion momentum distributions in ion-atom ionization by considering the three-body kinematics. Using the continuum distorted wave–eikonal initial state (CDW-EIS) approximation [9], it was shown how the most important ionization mechanisms in fast ion-atom collisions can be identified from the recoil-ion momentum distributions. These include: electron capture into the projectile continuum (ECC) [10–12], the emission of soft electrons (SE) [13], and projectile-electron binary collisions [14]. The analysis was demonstrated for single ionization of He by protons [8] and

by highly charged Ni²⁴⁺ ions [15]. The only other published “non-CTMC” calculations were done in 1991 by Fukuda *et al.* [16] who used the first Born and the eikonal distorted-wave approximations to calculate the recoil-ion momentum distributions. Recently the CDW-EIS method was also used by O’Rourke, Shinamura, and Crothers to analyze the transverse recoil-ion energy distribution [17]. However, none of these calculations addressed the important consequences of three-body kinematics on longitudinal recoil-ion momentum distributions that were detailed in [8].

While the major features of ionization dynamics at high velocities are relatively well understood [18,19], mechanisms of ionization at intermediate to low energies and by highly charged ions are still a subject of great controversy. In the low-energy region, ionization is a rather weak process compared with the dominant charge transfer. This is also the region where the Coulomb interactions among the three charged particles in the final state are expected to play an important role. In terms of total ionization cross sections, ionization of one-electron targets by protons and by highly charged ions has been addressed using the adiabatic electron superpromotion model [20–22] and by the extensive two-center close-coupling method of Wang *et al.* [23]. Experimental data on the momentum distributions of the ionized electrons will undoubtedly be useful to help better clarify the validity of the theoretical models and to provide insights into the importance of final-state interactions among the three charged particles.

In this paper, the analysis of recoil-ion momentum distribution reported in [8] is further developed. Our goal is to give a complete determination of the final-state momentum distributions for the electron, the projectile, and the target recoiling ions. From these distributions, we identify and describe the important features of the ionization dynamics. The method is used to analyze the recent measurements by Dörner *et al.* [6] and by Kravis *et al.* [7] for momentum distributions of the recoil ions and electrons in the single ionization of helium atoms. Comparisons with other theoretical approaches are made wherever available. Throughout this

*Electronic address: ydwang@phys.ksu.edu

†Electronic address: vladimir@chico.df.uba.ar

‡Permanent address: Department of Physics, Kansas State University, Manhattan, KS 66506-2601.

paper, atomic units are used unless otherwise stated.

II. THEORY

A. The quintuply differential cross sections

The most detailed information about single ionization of atoms by heavy-ion impact can be obtained experimentally from the measurement of five of the nine momentum components for the three particles in the final state. The other four components can be deduced from energy and momentum conservation of the three particles. Naturally there are numerous ways to define the quintuply differential cross sections. One choice that has been studied extensively in ion-atom ionizing collisions is the quintuply differential cross section in projectile scattering angle (Ω_p) and the ejected electron energy (ε_e) and angle (Ω_e):

$$\frac{d^5\sigma}{d\Omega_p d\varepsilon_e d\Omega_e} = \frac{\mu^2}{4\pi^2} |T_{if}|^2, \quad (1)$$

where T_{if} is the transition matrix, and μ is the reduced mass. Equation (1) is given in the center-of-mass frame. For heavy-ion collisions, we may also introduce

$$\frac{d^5\sigma}{d\vec{\eta} d\vec{p}_e} = \frac{1}{4\pi^2 v^2} |T_{if}|^2, \quad (2)$$

the quintuply differential cross section relating the transverse momentum transfer ($\vec{\eta}$) and the electron momentum (\vec{p}_e). Here \vec{v} is the velocity of the projectile and the momentum transfer is $\vec{P}_p = \vec{K}_i - \vec{K}_f = \vec{P}_p \cdot \vec{v} + \vec{\eta}$, where \vec{K}_i (\vec{K}_f) is the initial (final) momentum of the projectile. Integrating over Ω_p ($\vec{\eta}$), we can obtain the doubly differential cross section in electron energy (momentum) and angle.

In this paper, our goal is to study the momentum distributions of the recoiling ion and the electron. It is thus desirable to consider a quintuply differential cross section relating the recoil-ion momentum \vec{p}_R and the electron momentum \vec{p}_e . Below we obtain the quintuply differential cross section $d^5\sigma/d\vec{p}_{e\perp} d\vec{p}_{R\perp} dp_{R\parallel}$ from $d^5\sigma/d\vec{\eta} d\vec{p}_e$ by means of energy-momentum conservation.

The longitudinal momentum balance for the three particles along the incident beam direction,

$$p_{p\parallel} = p_{R\parallel} + p_{e\parallel} = Q/v = (\varepsilon_e - \varepsilon_i)/v, \quad (3)$$

where $p_{p\parallel}$ is the longitudinal momentum transfer of the projectile, $|\varepsilon_i|$ is the ‘‘binding energy’’ of the target atom in the initial state, and ε_e is the ejected electron energy. This equation is correct to $O(1/M_p)$ and $O(1/M_T)$, where M_p (M_T) is the mass of the heavy projectile (target). The fact that the longitudinal projectile momentum transfer is related to the Q value of the system leads to the simple transformation among longitudinal momentum distributions of the projectile, the electron and the recoiling ion. It also connects the longitudinal recoil-ion momentum distributions with the electron spectroscopy (DDCS) [8]. On the other hand, the transverse momentum conservation

$$\vec{\eta} = \vec{p}_{e\perp} + \vec{p}_{R\perp} \quad (4)$$

does not lead to any simple transformation. It would then be more convenient to obtain transverse momentum distributions from the T matrix. Details will be given later. Using Eqs. (3) and (4), we can show that

$$\frac{d^5\sigma}{d\vec{p}_{e\perp} d\vec{p}_{R\perp} dp_{R\parallel}} = \left| J \left(\begin{array}{c} \vec{\eta}, p_{e\parallel} \\ \vec{p}_{R\perp}, p_{R\parallel} \end{array} \right) \right| \frac{d^5\sigma}{d\vec{\eta} d\vec{p}_e}, \quad (5)$$

where the Jacobian $|J|$ is given by

$$J \left(\begin{array}{c} \vec{\eta}, p_{e\parallel} \\ \vec{p}_{R\perp}, p_{R\parallel} \end{array} \right) = \frac{v}{\sqrt{v^2 + 2\varepsilon_i + 2p_{R\parallel}v - p_{e\perp}^2}}. \quad (6)$$

This expression yields differential cross sections relating all three particles. The various forms of the quintuply differential cross sections introduced above are related to each other through the fundamental laws of energy and momentum conservations. They are directly related to the transition T matrix and can be used to derive a variety of differential cross sections of fewer dimensions.

‘‘Complete’’ experiments, where the momentum of each of the three particles in the final state is determined, are a standard technique in electron impact ionization studies (e - $2e$). For ion-atom collisions they only recently became feasible [24] and no fivefold differential cross sections have been published so far to our knowledge. However, much information on ionization dynamics can be obtained by studying differential cross sections concerning one or two of the three particles. In the following we derive some differential cross sections suitable for the description of final-state momentum distributions in ion-atom ionizing collisions.

B. Recoil-ion momentum distributions

Let us first consider the longitudinal recoil-ion momentum distributions, $d\sigma/dp_{R\parallel}$. From the energy-momentum conservation relation Eq. (3), we can show that the recoil-ion momentum distribution is related to the doubly differential cross section in electron energy and angle (DDCS) [8],

$$\frac{d\sigma}{dp_{R\parallel}} = \int_{\varepsilon_e^-}^{\varepsilon_e^+} \frac{1}{p_e} \frac{d^2\sigma}{d\varepsilon_e d(\cos\theta_e)} d\varepsilon_e, \quad (7)$$

where the lower and upper integration limits are implicitly given by [also from Eq. (3)]

$$p_e^\pm = v \cos\theta_e \pm \sqrt{v^2 \cos^2\theta_e + 2(p_{R\parallel}v - |\varepsilon_i|)} \quad (8)$$

and $\varepsilon_e^\pm = \frac{1}{2}(p_e^\pm)^2$.

The basic kinematic relation given in Eq. (3) imposes a severe constraint on the longitudinal momentum distribution in ion-atom ionization. In [8], Rodríguez, Wang, and Lin first pointed out that there is a kinematic threshold in the longitudinal recoil-ion momentum distribution given by

$$p_{R\parallel}^{\min} = -\frac{v}{2} + \frac{|\varepsilon_i|}{v}. \quad (9)$$

At $p_{R\parallel} = p_{R\parallel}^{\min}$ electrons are emitted at zero degrees with the same velocity v as the projectile. This corresponds to electron capture into the projectile continuum (ECC). The ECC

electrons are characterized as a cusp (Coulomb divergence) in the zero-degree DDCS spectroscopy. In the longitudinal recoil-ion momentum distribution, however, these electrons contribute to a finite cross section. This can be understood since the upper and lower integration limits in Eq. (7) approach the same value at ECC (i.e., $p_e^+ = p_e^- = v$). Measurements on the longitudinal recoil-ion momentum distributions can therefore provide unambiguous evidence for the ECC ionization mechanism.

We now turn to the transverse recoil-ion momentum distribution $d\sigma/dp_{R\perp}$. Using the quintuply differential cross section introduced in Eq. (5) we can see that the transverse recoil-ion momentum distribution is expressed as

$$\frac{d\sigma}{dp_{R\perp}} = 2\pi p_{R\perp} \int d\vec{p}_{e\perp} \int_{-\infty}^{\infty} dp_{R\parallel} \frac{d^5\sigma}{d\vec{p}_{e\perp} d\vec{p}_{R\perp} dp_{R\parallel}}. \quad (10)$$

The kinematic relation of Eq. (4) will be used to carry out the integrations. It should be pointed out that projectile-target internuclear interaction is known to make an important contribution to the projectile angular distribution. It also affects the transverse recoil-ion momentum distribution.

C. Electron momentum distributions

Experiments on electron momentum distributions in coincidence with recoil-ion momentum distribution have only been done very recently. Kravis *et al.* [7] measured electron momentum distributions in single ionization of He by protons and by C^{6+} ions at low to intermediate energies. Moshhammer *et al.* [5] measured longitudinal electron momentum distributions in single ionization of He by highly charged Ni^{24+} ions. Theoretically, both the longitudinal and the transverse electron momentum distributions can be obtained directly from the DDCS or from the transition T matrix.

For a given $p_{e\parallel}$, the longitudinal electron momentum distribution $d\sigma/dp_{e\parallel}$ can be obtained by integrating the DDCS over the electron energy,

$$\frac{d\sigma}{dp_{e\parallel}} = \int_{p_{e\parallel}^2/2}^{\infty} \frac{1}{p_e} \frac{d^2\sigma}{d\varepsilon_e d(\cos\theta_e)} d\varepsilon_e. \quad (11)$$

The integral is regular everywhere except at the ECC where $p_{e\parallel} \rightarrow v$. In the neighborhood of $p_{e\parallel} = v$, the derivative of $d\sigma/dp_{e\parallel}$ is discontinuous. The change of slope across $p_{e\parallel} = v$ arises from the behavior of the DDCS at the ECC.

The transverse electron momentum distribution is not influenced by the internuclear interaction. One can obtain $d\sigma/dp_{e\perp}$ from the DDCS,

$$\frac{d\sigma}{dp_{e\perp}} = \int_{p_{e\perp}^2/2}^{\infty} \frac{1}{p_e} \frac{p_{e\perp}}{p_e} \frac{d^2\sigma}{d\varepsilon_e d(\cos\theta_e)} d\varepsilon_e, \quad (12)$$

where $p_{e\parallel}^2 + p_{e\perp}^2 = 2\varepsilon_e$. In the experiment of Kravis *et al.* [7], the momentum projection along the y axis was also measured. The y -direction electron momentum distribution can be obtained by

$$\frac{d\sigma}{dp_{ey}} = \int_{-\infty}^{+\infty} dp_{ex} \int_{-\infty}^{+\infty} \frac{d\sigma}{d\vec{p}_e} dp_{ez}, \quad (13)$$

where

$$\frac{d\sigma}{d\vec{p}_e} = \int d\vec{\eta} \frac{d^5\sigma}{d\vec{\eta} d\vec{p}_e}. \quad (14)$$

The perpendicular distribution $d\sigma/dp_{ey}$ is symmetric about $p_{ey} = 0$.

D. Projectile momentum transfer distributions

The longitudinal projectile momentum transfer distribution $d\sigma/dp_{P\parallel}$ is simply related to the singly differential cross section of the ejected electron:

$$\frac{d\sigma}{dp_{P\parallel}} = v \frac{d\sigma}{d\varepsilon_e}. \quad (15)$$

From Eq. (3), the longitudinal projectile momentum distribution starts at $p_{P\parallel} = |\varepsilon_i|/v$, corresponding to zero-energy electron emission. For fast collisions, the longitudinal projectile momentum transfer distribution decreases with increasing $p_{P\parallel}$. The distribution resembles the single differential cross section in electron energy. Since $p_{P\parallel}$ is related to the collision Q value ($p_{P\parallel} = Q/v$), the longitudinal projectile momentum transfer is a measure of the overall inelasticity of the collision process.

The transverse projectile momentum transfer distribution $d\sigma/dp_{P\perp}$ follows from Eq. (2),

$$\frac{d\sigma}{dp_{P\perp}} = 2\pi p_{P\perp} \int d\vec{\eta} \frac{d^5\sigma}{d\vec{\eta} d\vec{p}_e}, \quad (16)$$

where $\vec{\eta} = p_{P\perp}^*$. Collision dynamics on the transverse projectile momentum distribution may be obtained from the conventional measurement of the projectile scattering angle θ_P since $\eta \approx \mu v \theta_P$, for small θ_P . However, measurement of the projectile angular distribution in fast ion-atom collisions is quite difficult because of the extremely small deflection of the projectile [25–28]. On the other hand, it is much easier to measure the transverse recoil-ion and ejected electron momenta. The conservation of transverse momentum in Eq. (4) can be used to extract information on projectile transverse momentum.

III. RESULTS AND DISCUSSION

The formulation outlined in Sec. II is quite general and independent of theoretical model(s) used for evaluating the transition T matrix. However, no exact solution for three-body breakup is available. In this paper we employed the CDW-EIS approximation of Crothers and McCann [9] to evaluate T_{if} . The CDW-EIS model has the salient feature that the ionized electron sees the Coulomb field from both the target and the projectile ions. The wave functions employed by the CDW-EIS satisfy the correct asymptotic boundary conditions of the Coulombic three-body problem. This model includes effects due to the long-range nature of the target and the projectile interactions in the entrance and

exit channels. It has been proven to be quite successful in describing the ionization of atoms by protons, antiprotons and by highly charged ions. Concerning the details of this method and its application to the study of ejected electron spectroscopy, a review has been given by Fainstein, Ponce, and Rivarola [19].

The standard CDW-EIS approximation of Crothers and McCann [9] was developed for ionization of a hydrogenic atom by a bare ion. Following the work of Fainstein, Ponce, and Rivarola [29], we used an independent electron model to treat the two-electron helium target. The initial target atomic state is described by the Hartree-Fock wave function and the final state is given by the hydrogenic wave function with an effective charge. We could have also adopted the recent approach of Gulyás, Fainstein, and Salin [30] who replaced the hydrogenic final Coulomb function with numerical continuum wave functions obtained from the Hartree-Fock potential. The advantage would be that the continuum functions are orthogonal to the bound ones. However, the use of numerical wave functions will make the evaluation of multiple integrals in the momentum distributions more complicated and the main features of the results are not expected to change due to this improvement.

The independent electron model adopted here is basically identical to what has been in use for treating single-electron processes in collisions with multielectron targets (cf. [31]). The model is expected to be less applicable for collisions at lower energies. For the dominant collision process this is expected to be valid to the first order. The present model adopts the same approximation, with the emphasis on the momentum distribution of the collision products.

In this paper we also evaluated T_{if} using the first Born approximation [32]. Comparison between the CDW-EIS and the first Born approximation is used to demonstrate the importance of including the long-range projectile ion-target electron interaction in the final state.

In the following we present detailed results for final-state momentum distributions in the ionization of helium by protons and by some highly charged ions for which the measurements have been done. In carrying out the CDW-EIS and the first Born calculations, we used two different effective charges Z_T . The first is $Z_T=1.344$, arising from the ionization potential of the He atom ($\varepsilon_i = -0.903$ a.u.). The second is the variational charge $Z_T=1.688$. Magnitudes of the cross sections obtained from the two effective charges generally differ by no more than 20%. For clarity of the presentation, we present results obtained with $Z_T=1.344$.

A. Longitudinal recoil-ion momentum distributions

At intermediate to high collision energies, Dörner *et al.* [6] measured the longitudinal recoil-ion momentum distributions in single ionization of He by fast protons. In Fig. 1, we compare their measurements with the present CDW-EIS and first Born calculations for ionization of He by protons at 0.25, 0.5, and 1 MeV. The overall agreement between the calculations and measurements is excellent.

The longitudinal recoil-ion momentum distributions at the three energies shown in Fig. 1 have similar shapes. Each distribution shows a single peak centered around $p_{R||}=0$. Cross sections drop rapidly on both sides of the peak. It is

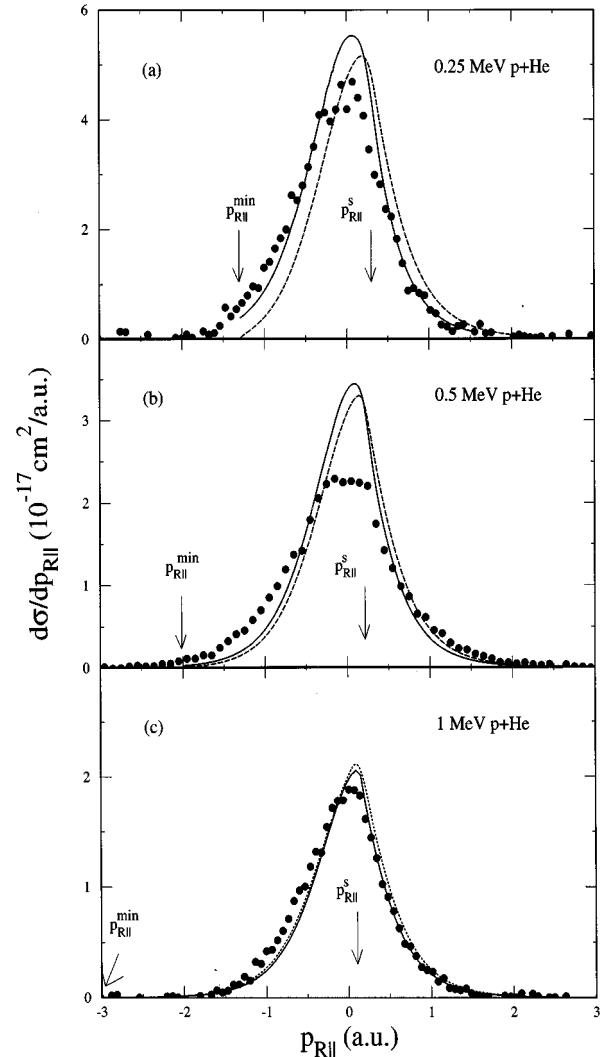


FIG. 1. Longitudinal recoil-ion momentum distribution for single ionization of He by protons at (a) 0.25, (b) 0.5, and (c) 1 MeV. Experimental data are from Dörner *et al.* [6]. Solid line: present CDW-EIS calculation; dashed line: present first Born calculation. Arrows indicate the positions of $p_{R||}^s$ and $p_{R||}^{\min}$ (see text). (a) $p_{R||}^s=0.29$ a.u., $p_{R||}^{\min}=-1.30$ a.u.; (b) $p_{R||}^s=0.20$ a.u., $p_{R||}^{\min}=-2.03$ a.u.; (c) $p_{R||}^s=0.14$ a.u., $p_{R||}^{\min}=-3.02$ a.u..

clear that the peak in the longitudinal recoil-ion momentum distribution corresponds to the emission of low-energy electrons. These so-called SE are most important in the total ionization cross section. Results shown in Fig. 1 reflect the importance of soft-electron emission from the perspective of recoil-ion momentum distributions.

The peak position in the longitudinal recoil-ion momentum distribution needs more detailed analysis. Since we have identified the peak as being due to the emission of soft electrons, we would expect the peak position at $p_{R||}=p_{R||}^s=|\varepsilon_i|/v$, which corresponds to the extreme situation in Eq. (3) where electrons are emitted with zero energies. If this were true, we would expect that the peak position for ionization of He by 0.25-, 0.5-, and 1-MeV protons would appear at 0.29, 0.20, and 0.14 a.u., respectively. However, a careful observation of Fig. 1 shows that the peak position in the longitudinal recoil-ion momentum distribution is generally shifted to a lower value of $p_{R||}$. The distribution is thus

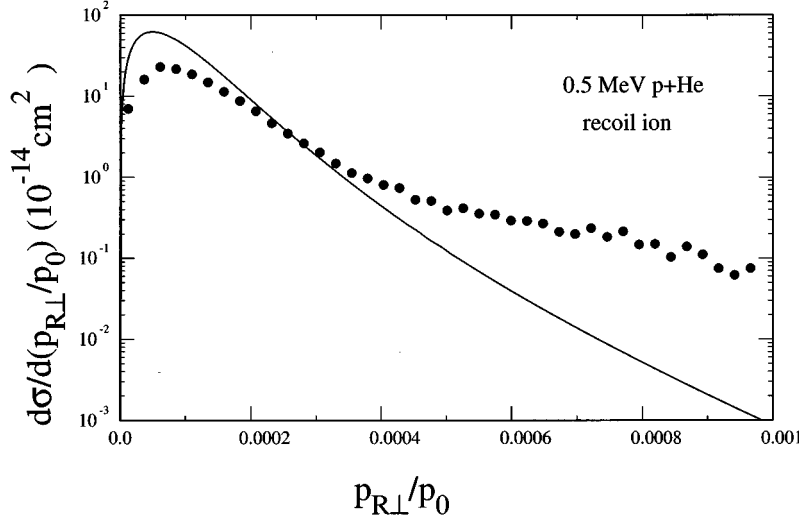


FIG. 2. Transverse recoil-ion momentum distribution for single ionization of He by protons at 0.5 MeV. Experimental data are from Dörner *et al.* [6]. Solid line: present CDW-EIS calculation.

backward shifted. In fact, the momentum distributions at the three collision energies are all peaked near $p_{R\parallel}=0$. The enhancement of the longitudinal recoil-ion momentum distribution in the backward direction is due to the enhancement of low-energy electrons emitted in the forward direction. The enhancement of forward low-energy electrons is a well-known phenomenon in electron spectroscopy and has been studied in both theory and experiment [13,33].

In Fig. 1, the peak position predicted by the CDW-EIS theory is in excellent agreement with the experimental observation. We note that the simple first Born approximation also predicted a backward shift in the longitudinal recoil-ion momentum distribution although the magnitude of the shift is too small. This is not surprising. The first Born approximation is known to partially account for the enhancement of electrons emitted in the forward direction [33]. With the increase of projectile energy, the backward enhancement of the longitudinal recoil-ion momentum distribution decreases and the peak position moves to $p_{R\parallel}^s$. Also, the difference between the CDW-EIS and first Born approximations diminishes with increasing projectile velocity.

In Sec. II, we pointed out that there is a kinematic threshold characterizing the electron capture into projectile continuum in the longitudinal recoil-ion momentum distribution. In Fig. 1, we can identify the kinematic threshold according to Eq. (3). At 0.25 MeV, we can see a clear threshold at $p_{R\parallel}^{\min} = -1.296$ from the CDW-EIS calculation. The measured data below this value could be ascribed to background noise and should be discarded. At higher energies, the cross section near the threshold becomes much smaller. There is not enough statistics in the data to indicate the threshold. Since the ECC threshold is a pure kinematic effect, it cannot depend on the projectile charge. In the same paper, Dörner *et al.* [6] also reported measurement for ionization of He by He^{2+} ions at 0.25 MeV/amu. The threshold occurs at the same $p_{R\parallel}$ as in the ionization by 0.25-MeV protons.

Dörner *et al.* reported calculations using the classical trajectory Monte Carlo (*n*CTMC) method [6]. The peak position for the longitudinal momentum distribution predicted by the *n*CTMC is consistently shifted to *smaller* $p_{R\parallel}$ as compared with the experiment. In other words, the *n*CTMC predicted an even larger backward shift in the longitudinal mo-

mentum distributions than the CDW-EIS theory and the experiment. Furthermore, the agreement between *n*CTMC and the experiment does not seem to improve as the projectile energy is increased. In fact, the *n*CTMC shows the worst agreement with the experiment at 1 MeV, which is the highest collision energy measured. In our calculations, the CDW-EIS approaches the first Born approximation with increasing projectile velocity. The agreement with the experiment is also improved at higher energies. Our integrated total ionization cross sections at the three collision energies are in good agreement with those reported by Shah and Gilbody [37].

Dörner *et al.* [6] also reported the longitudinal recoil-ion momentum distributions at a given transverse recoil-ion momentum. We will discuss this measurement in Sec. III B.

B. Transverse recoil-ion momentum distributions

The transverse momentum distribution in ion-atom ionization represents a delicate energy-momentum balance among all collision particles [see Eq. (4)]. The measurement of the transverse recoil-ion momentum distribution can probe the impact parameter dependence of the collision process. Previously, our understanding of transverse momentum balance was largely based on measurements of projectile angular distributions (cf. [25–28]). Such measurements are undoubtedly quite difficult at high velocities. With recent progress in recoil-ion momentum spectroscopy, it has become possible to measure the transverse recoil-ion momentum distribution.

In Fig. 2, we compare our calculations with the recent measurement of Dörner *et al.* [6] for single ionization of He by 0.5-MeV proton impact. The transverse recoil-ion momentum distribution is presented as a function of the ratio between the transverse-recoil ion momentum ($p_{R\perp}$) and the initial projectile momentum ($p_0 = M_p v$). There is a relatively large difference between the theory and the measurement at large $p_{R\perp}$. This is expected because the standard CDW-EIS formulation [9] does not include the internuclear interaction between the projectile and the target nucleus. In the previous calculations on the projectile angular distribution, it was shown that projectile-target internuclear interaction makes an important contribution at large scattering

angles [16,35,36]. The projectile-target internuclear interaction accounts for projectile angular distributions beyond the critical angle $\theta_p^c = 0.55$ mrad representing the maximum scattering angle for a proton being deflected by an electron at rest in a binary projectile-electron collision. In the case of the transverse recoil-ion momentum distribution, however, the role of projectile-target internuclear interaction is less clear because of the delicate momentum balance Eq. (4) among the three particles in the final state. In Fig. 2, it does not seem to be obvious to identify a region where the internuclear interaction is more important although discrepancies between the present CDW-EIS theory and the measurement increase with increasing $p_{R\perp}$.

In Fig. 3, we compare the calculated longitudinal recoil-ion momentum distributions for various transverse momenta ranging from $p_{R\perp} = 0$ to 7 a.u. with the measurement of Dörner *et al.* [6] for $p + \text{He}$ ionization at 0.5 MeV. Our calculations show similar dependence on transverse momentum as observed in the experiment. Cross sections decrease rapidly with increasing transverse momentum. The observed momentum distributions are well described by the present theory for $p_{R\perp}$ between 0 and 3 a.u. The agreement between theory and experiment becomes worse with increasing $p_{R\perp}$, indicating again the increasing importance of the internuclear interaction. Experimental uncertainties also increase with $p_{R\perp}$. In Fig. 3, the ECC mechanism is shown in the calculations as a finite value at the kinematic threshold $p_{R\parallel}^{\text{min}} = -2.034$ a.u. We point out that at the ECC, the transverse recoil-ion momentum $\vec{p}_{R\perp}$ exactly balances off the transverse projectile momentum transfer $\vec{\eta}$ since $\vec{p}_{e\perp} = 0$. The broadening in the momentum distribution shown by the experimental results is also present in the theoretical calculations. It follows from the increasing importance of the finite value at threshold. Dörner *et al.* reported the n CTMC calculations for their measurements [6]. The n CTMC results also show large discrepancy with experiment on the shape of the longitudinal momentum distribution at large $p_{R\perp}$. It does, however, reproduce the single differential cross section as a function of recoil transverse momentum quite well, since it includes the internuclear interactions classically.

C. Electron momentum distribution

At high velocities, Dörner *et al.* [6] extracted the transverse electron momentum distribution $d\sigma/dp_{e\perp}$ in single ionization of He by 0.5-MeV protons from the doubly differential electron spectra measured by Rudd, Toburen, and Stolterfoht [37]. In Fig. 4, both the CDW-EIS and the first Born calculations agree with the data quite well since the projectile energy is sufficiently high. It should be pointed out that this distribution is calculated from the DDCS [see Eq. (12)], and therefore does not depend on the inclusion of the internuclear interaction in the calculations. This is true since the DDCS are obtained by integrating over the projectile scattering angles. In the figure we can see there is a change of slope at $p_{e\perp}/p_0 \approx 0.5 \times 10^{-3}$. This is also related to the critical scattering angle $\theta_p^c \approx 0.55$ mrad. In this limit case the ejected electron carries out a transverse momentum $p_{e\perp} = v$. Beyond that point the projectile-electron binary collision mechanism cannot contribute and the distribution decreases quickly.

At low to intermediate energies, Kravis [7] measured both longitudinal and transverse electron momentum distributions in single ionization of He by protons and C^{6+} at projectile velocities between 1 and 2 a.u. These measurements provide

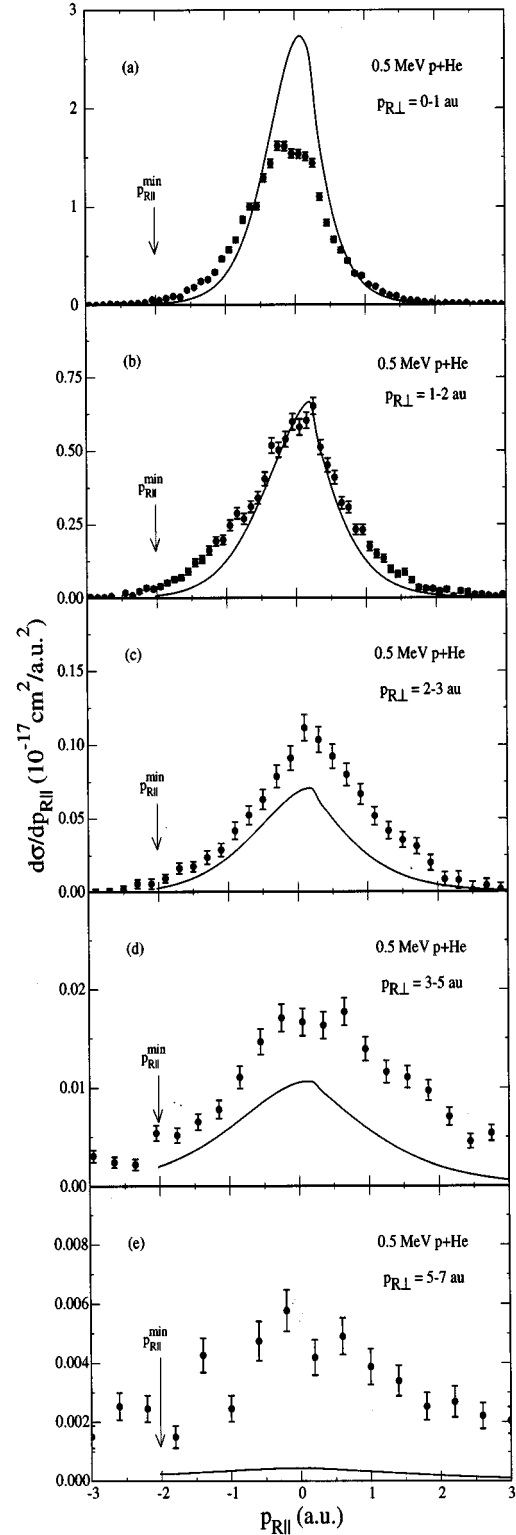


FIG. 3. Longitudinal recoil-ion momentum distribution for single ionization of He by 0.5-MeV protons for various transverse recoil-ion momenta. Experimental data are from Dörner *et al.* [6]. Solid line: present CDW-EIS calculation. Arrows indicate the $p_{R\parallel}^{\text{min}}$ threshold at -2.03 a.u.

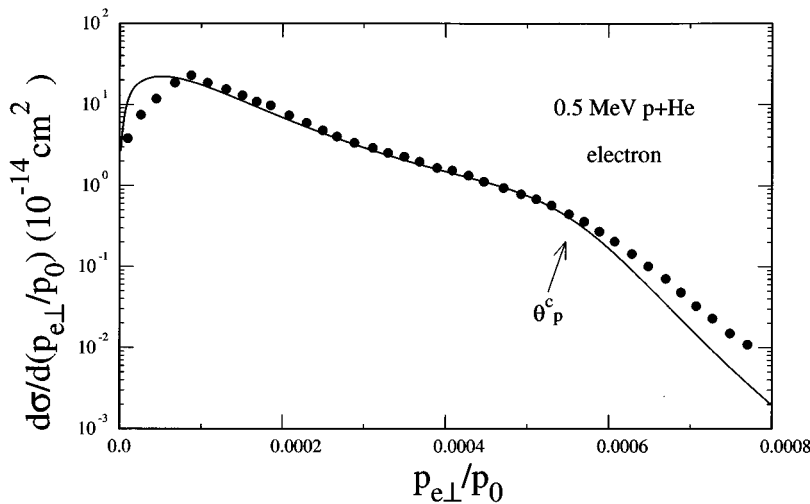


FIG. 4. Transverse electron momentum distribution for single ionization of He by protons at 0.5 MeV. Experimental data are from Rudd, Töburen, and Stolterfoht [37] as quoted in Dörner *et al.* [6]. Solid line: present CDW-EIS calculation. $\theta_p^c \approx 0.55$ mrad is the critical scattering angle (see text).

information on the momentum space distribution of the ionized electrons in the presence of two Coulomb potentials. Below we focus on the longitudinal electron momentum distribution.

In Fig. 5, we compare the CDW-EIS and the first Born calculations for the longitudinal electron momentum distributions $d\sigma/dp_{e\parallel}$ in ionization of He by protons at $v = 2.39, 1.71,$ and 1.15 a.u. (or $E = 143, 73,$ and 33 keV). Though the Born approximation is not supposed to be valid at such low energies, it is interesting to see how it does in predicting the momentum distributions. For ionization of He by protons, the CDW-EIS theory is shown to be able to give accurate total cross sections [9,19] at energies as low as 30 keV. The present CDW-EIS calculations agree very well with the measurements. Most importantly, the CDW-EIS theory correctly predicts the peak position in the electron momentum distribution at the three energies. The peak position predicted by the first Born approximation is almost independent of the projectile velocity, indicating that it does not include the final-state interactions. We should point out that even the Born approximation does not give the peak position at $p_{e\parallel} = 0$. That would be the case only if the soft electrons are emitted isotropically. This fact is also reflected in the description of the longitudinal recoil-ion momentum distribution where the first Born approximation resulted in a backward shift (see Sec. III B).

The contribution of the so-called ECC electrons is centered precisely at $p_{e\parallel}/v = 1$ in Fig. 5 in the CDW-EIS calculations. These electrons are ejected with the same velocity as the projectile. They result in a “kink” (change of slope) in the momentum distribution at v . The “kink” in the theoretical calculations is quite clear at $v = 2.39$ and 1.71 a.u. At $v = 1.15$ a.u., the projectile velocity is rather small and the ECC electron contribution is mixed with that of the soft electrons. Figure 5 shows that the parallel component of the electron momentum falls most likely between the projectile and the target. This latter observation is more obvious at low velocities (e.g., $v = 1.71$ and 1.15 a.u.). The reasonably good agreement between the CDW-EIS and the measurement regarding the shape and location of the electron momentum distribution shows that the CDW-EIS can provide a qualitative description of the main features of three-body ionization dynamics.

We now turn to the ionization of He by highly charged ions at comparable velocities. In [7], longitudinal electron momentum distributions were measured for ionization of He by C^{6+} ions at $v = 1.63, 1.38,$ and 1.16 a.u. This is the low-energy region where the cross section for electron transfer is larger than that of ionization by two orders of magnitude [38,39]. The CDW-EIS model is not expected to work in this energy region and for these collision systems since the effect of charge transfer on the ionization is not explicitly included in the perturbative treatment. Below the CDW-EIS model was used to check how much the so-called “two-center” effect is reflected in such collision systems.

In Fig. 6, we show the CDW-EIS cross sections normalized to the peaks of the measured distributions. The shapes of the momentum distributions are only moderately represented by the CDW-EIS except at the highest velocity $v = 1.63$. In all cases, the CDW-EIS tend to highlight the importance of projectile center or the ECC mechanism while the first Born theory predicts that most electrons should be emitted around the target center. The three distributions shown in Fig. 6 for ionization by C^{6+} seem to have quite different velocity dependences from the corresponding distributions for proton impact ionization. The “pulling” of electrons towards the highly charged projectile may indicate a strong post-collision effect. In the case of proton impact, such effects are weaker because of the lower projectile charge.

In a recent calculation for total ionization of He by C^{6+} using the two-center close-coupling method, Wang *et al.* [23] found that the projectile center plays an important role. Within the same two-center basis set, projectile continuum states become more important with increasing velocity. The increasing importance of the projectile center was used to explain the observed strong onset in the ionization cross section observed by Wu *et al.* [38]. With decreasing velocity, the target center will eventually become important. We must keep in mind that this conclusion is obtained for low-energy ionization by highly charged ions, where the ionization probability is extremely small. When compared with the close-coupling calculation [23], the CDW-EIS often overestimates the total ionization cross section by about a factor of 2 [in Figs. 6(a) and 6(b)]. At the lowest collision velocity shown in Fig. 6(c), however, the CDW-EIS underestimates the total

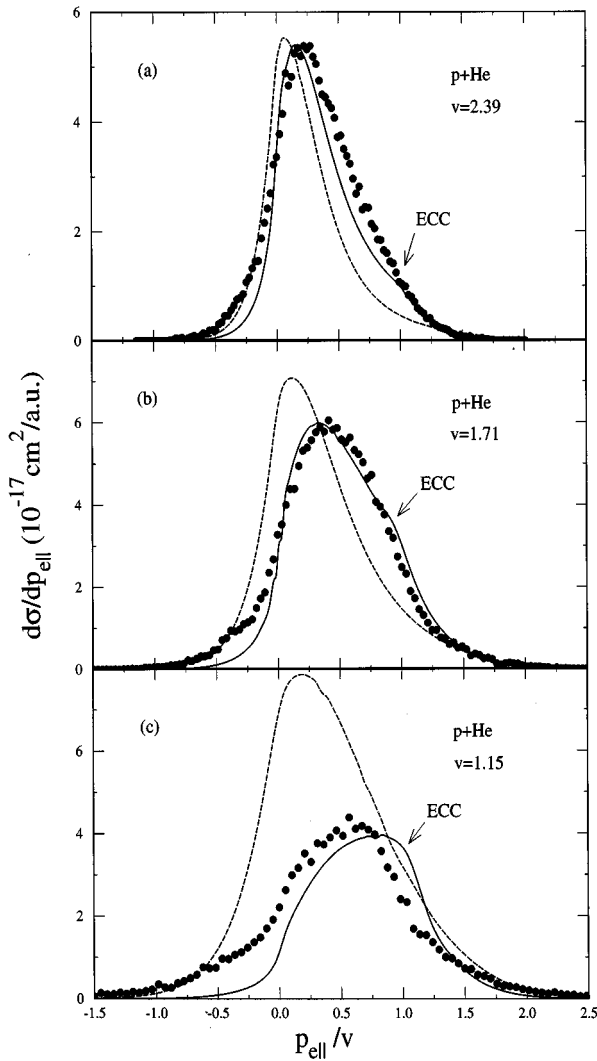


FIG. 5. Longitudinal electron momentum distribution as function of $p_{e\parallel}/v$ for ionization of He by protons at intermediate to low velocity: (a) $v=2.39$ a.u.; (b) $v=1.71$ a.u.; and (c) $v=1.15$ a.u. Experimental data are from Kravis *et al.* [7]. Solid line: present CDW-EIS calculation; dashed line: present first Born calculation.

cross section by about a factor of 2, reflecting the rapid change of the total cross section at these low velocities.

Finally, we note that the discrepancy between the CDW-EIS and the measurement on ionization of He by highly charged ions is not because of the use of independent electron model for treating the two-electron target. As demonstrated by Wang *et al.* [23] in their close-coupling calculations, the independent electron approximation works rather well in predicting single ionization and single charge transfer cross sections in the $C^{6+} + \text{He}$ collision system in the present velocity region.

IV. CONCLUSIONS

In this paper we have formulated a quantum mechanical theory for describing the momentum distributions in ion-atom single ionization. Our formulation is quite general and is independent of the collision model used for calculating the transition matrix. The energy-momentum balance among the three particles is used to extract a variety of differential cross

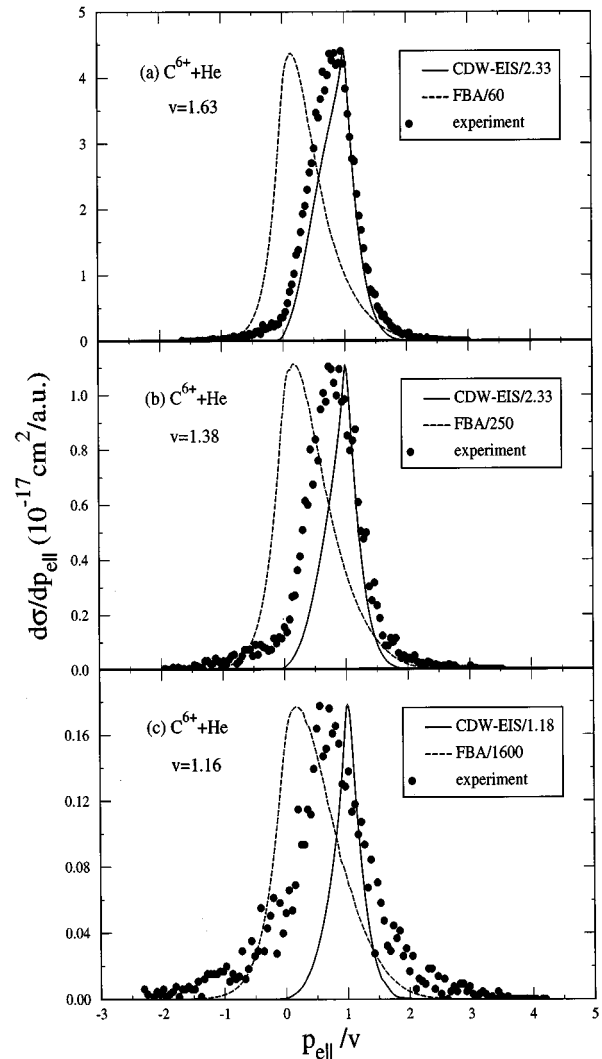


FIG. 6. Longitudinal electron momentum distribution as function of $p_{e\parallel}/v$ for ionization of He by C^{6+} highly charged ions at low velocity: (a) $v=1.63$ a.u.; (b) $v=1.38$ a.u.; and (c) $v=1.16$ a.u. Experimental data are from Kravis *et al.* [7]. Solid line, present CDW-EIS calculation; dashed line, present first Born calculation (FBA). The calculations are normalized to experimental peak values.

sections. The three prominent features in ion-atom ionization process (i.e., soft electron emission, electron capture into the projectile continuum, and projectile-electron binary collision) can all have signatures in the final-state momentum distributions of the projectile, the electron, and the recoiling ion. Collisions at both high and low velocities and by both low and highly charged projectiles were considered in this paper. The standard CDW-EIS theory was applied to calculate the cross sections. This theory accounts for the long-range interaction of the projectile and target Coulomb field. As a comparison, the first Born approximation, which does not take into account these refinements, was also applied. The comparison between the CDW-EIS and the Born approximations shows the importance of two-center effects. In general, the CDW-EIS theory is able to identify and describe the main features of ionization dynamics. It gives both qualitative and quantitative descriptions for final-state momentum distributions in the single ionization of He by protons at intermediate to low energies.

ACKNOWLEDGMENTS

We are grateful to D.S.F. Crothers and O'Rourke for useful discussions. We also acknowledge discussions with P. Richard, L. Tribedi, and J. Ullrich. This work is supported by the Division of Chemical Sciences, Office of Basic Energy

Sciences, Office of Energy Research, U.S. Department of Energy. V.D.R. has been partially supported by the Consejo Nacional de Investigaciones Científicas y Técnicas under PID 3357/92-CONICET (ARGENTINA). R.D. was supported by the Alexander von Humboldt Stiftung.

-
- [1] J. Ullrich, R.E. Olson, R. Dörner, V. Dangeredorf, S. Kelbch, H. Berg, and H. Schmidt-Böcking, *J. Phys. B* **22**, 627 (1989).
- [2] R. Dörner, R.E. Olson, and H. Schmidt-Böcking, *Phys. Rev. Lett.* **63**, 147 (1989).
- [3] R. Ali, V. Frohne, C.L. Cocke, M. Stöckli, and M. Raphaeliam, *Phys. Rev. Lett.* **69**, 2491 (1992).
- [4] V. Frohne, S. Cheng, R. Ali, M. Raphaeliam, C.L. Cocke, and R.E. Olson, *Phys. Rev. Lett.* **71**, 696 (1993).
- [5] R. Moshhammer, J. Ullrich, M. Unverzagt, W. Schmidt, P. Jardin, R.E. Olson, R. Mann, R. Dörner, V. Mergel, U. Buck, and H. Schmidt-Böcking, *Phys. Rev. Lett.* **73**, 3371 (1994).
- [6] R. Dörner, V. Mergel, L. Zaoyuan, J. Ullrich, L. Spielberger, R.E. Olson, and H. Schmidt-Böcking, *J. Phys. B* **28**, 435 (1995).
- [7] S. Kravis *et al.* (unpublished).
- [8] V.D. Rodríguez, Y.D. Wang, and C.D. Lin, *Phys. Rev. A* **52**, R9 (1995).
- [9] D.S.F. Crothers and J.F. McCann, *J. Phys. B* **16**, 3229 (1983).
- [10] G.B. Crooks and M.E. Rudd, *Phys. Rev. Lett.* **25**, 1599 (1970).
- [11] K.G. Harrison and M. Lucas, *Phys. Lett.* **33A**, 149 (1970).
- [12] M.W. Lucas and W. Steckelmacker, in *Proceedings of the Third Workshop on High-Energy Ion-Atom Collisions, Debrecen, Hungary, 1987*, edited by D. Berenyi and G. Hock, *Lecture Notes in Physics* Vol. 294 (Springer-Verlag, Berlin, 1987), p. 229.
- [13] S. Suárez, C. Garibotti, W. Meckbach, and G. Bernardi, *Phys. Rev. Lett.* **70**, 418 (1993).
- [14] D.H. Lee, P. Richard, T.J.M. Zourus, J.M. Sanders, J.L. Sinpaugh, and H. Hidmi, *Phys. Rev. A* **41**, 4816 (1990).
- [15] V.D. Rodríguez, Y.D. Wang, and C.D. Lin, *J. Phys. B* **28**, L471 (1995).
- [16] H. Fukuda, I. Shimamura, L. Végh, and T. Watanabe, *Phys. Rev. A* **44**, 1565 (1991).
- [17] S.F. O'Rourke, I. Shimamura, and D.S.F. Crothers, *Proc. R. Soc. London A* **452**, 175 (1996).
- [18] J.E. Miraglia and J. Macek, *Phys. Rev. A* **43**, 5919 (1991).
- [19] P.D. Fainstein, V.H. Ponce, and R.D. Rivarola, *J. Phys. B* **24**, 3091 (1991).
- [20] E.A. Solov'ev, *Zh. Eksp. Teor. Fiz.* **81**, 1681 (1981) [*Sov. Phys. JETP* **54**, 893 (1981)].
- [21] J.H. Macek and S.Y. Ovchinnikov, *Phys. Rev. A* **50**, 468 (1994).
- [22] R.K. Janev, G. Ivanovski, and E.A. Solov'ev, *Phys. Rev. A* **49**, R645 (1994).
- [23] Y.D. Wang, C.D. Lin, N. Toshima, and Z. Chen, *Phys. Rev. A* **52**, 2852 (1995).
- [24] R. Moshhammer, M. Unverzagt, W. Schmitt, J. Ullrich, and H. Schmidt-Böcking, *Rev. Sci. Instrum.* (to be published).
- [25] E.Y. Kamber, C.L. Cocke, S. Cheng, J.H. McGuire, and S.L. Varghese, *J. Phys. B* **21**, L455 (1988).
- [26] E.Y. Kamber, C.L. Cocke, S. Cheng, and S.L. Varghese, *Phys. Rev. Lett.* **60**, 2026 (1988).
- [27] F.G. Kristensen and E. Horsdal-Pedersen, *J. Phys. B* **23**, 4129 (1990).
- [28] G. Schiwietz, P. Grande, C. Auth, H. Winter, and A. Salin, *Phys. Rev. Lett.* **72**, 2159.
- [29] P.D. Fainstein, V.H. Ponce, and R.D. Rivarola, *J. Phys. B* **23**, 1481 (1990).
- [30] L. Gulyás, P.D. Fainstein, and A. Salin, *J. Phys. B* **28**, 245 (1995).
- [31] J.H. McGuire and O.L. Weaver, *Phys. Rev. A* **16**, 41 (1977).
- [32] D.R. Bates and G. Griffing, *Proc. Phys. Soc. A* **66**, 961 (1953).
- [33] D.H. Madison, *Phys. Rev. A* **8**, 2449 (1973).
- [34] M.B. Shah and H.B. Gilbody, *J. Phys. B* **18**, 899 (1985).
- [35] A. Salin, *J. Phys. B* **22**, 3901 (1989).
- [36] V.D. Rodríguez, *J. Phys. B* **29**, 275 (1996).
- [37] M.E. Rudd, L.H. Toburen, and N. Stolterfoht, *Nucl. Data Tables* **18**, 413 (1976).
- [38] W. Wu, C.L. Cocke, J.P. Giese, F. Melchert, M.L.A. Raphaelian, and M. Stöckli, *Phys. Rev. Lett.* **75**, 1054 (1995).
- [39] W. Wu, Ph.D. dissertation, Kansas State University, 1994.